The dissipated power in atomic force microscopy due to interactions with a capillary fluid layer

N. Hashemi, M. R. Paul, H. Dankowicz, M. Lee, and W. Jhe

The dissipated power in atomic force microscopy due to interactions with a capillary fluid layer

N. Hashemi,[1,a)] M. R. Paul,[1] H. Dankowicz,[2] M. Lee,[3] and W. Jhe[3]

[1]*Department of Mechanical Engineering, Virginia Polytechnic Institute and State University, Virginia 24061, USA*
[2]*Department of Mechanical Science and Engineering, University of Illinois at Urbana-Champaign, Illinois 61801, USA*
[3]*Department of Physics and Astronomy, Seoul National University, Seoul, 151-747, Republic of Korea*

We study the power dissipated by the tip of an oscillating micron-scale cantilever as it interacts with a sample using a nonlinear model of the tip-surface force interactions that includes attractive, adhesive, repulsive, and capillary contributions. The force interactions of the model are entirely conservative and the dissipated power is due to the hysteretic nature of the interaction with the capillary fluid layer. Using numerical techniques tailored for nonlinear and discontinuous dynamical systems we compute the exact dissipated power over a range of experimentally relevant conditions. This is accomplished by computing precisely the fraction of oscillations that break the fluid meniscus. We find that the dissipated power as a function of the equilibrium cantilever-surface separation has a characteristic shape that we directly relate to the cantilever dynamics. Even for regions where the cantilever dynamics are highly irregular the fraction of oscillations breaking the fluid meniscus exhibits a simple trend. Using our results we also explore the accuracy of the often used harmonic approximation in determining dissipated power. © *2008 American Institute of Physics.* [DOI: 10.1063/1.2980057]

Understanding the force interactions between the tip of an oscillating micron-scale cantilever and the surface of interest is central to dynamic atomic force microscopy (AFM).[1–3] Measurements of the amplitude, frequency, and phase of the oscillating cantilever have been widely used to probe surface properties. The relative phase difference between the cantilever tip and the drive quantifies the energy dissipated by the tip-surface interactions.[2,4–9] As a result, phase contrast measurements offer the potential to probe surface properties otherwise inaccessible or difficult to determine. In experiment, the dissipated power is often measured indirectly using the harmonic approximation of Cleveland *et al.*[4] In this approximation the cantilever dynamics are assumed to remain sinusoidal. The power dissipated by tip-surface interactions is measured as the difference between the power supplied and the power dissipated by elastic and viscous damping. The building of a quantitative link between the power dissipated and the surface properties requires a detailed understanding of the dissipation dynamics.[7–11] We explore the power dissipated in the presence of a hysteretic and conservative tip-sample interaction force where the source of hysteresis is the formation and rupture of a liquid bridge between the tip and sample.

The use of point-mass models with nonlinear, and often discontinuous, tip-surface force interactions has been very useful in providing physical insight into the complex dynamics tapping mode AFM.[12–17] We use the point-mass model of Zitzler *et al.*[17] that includes long-range attraction, adhesion, and repulsion forces as well as the interactions of capillary fluid layers covering both the tip and sample due to ambient

humidity.[18] We refer the reader to Ref. 17 for a detailed discussion of the model. We only provide the essential ingredients necessary for our discussion. The equation of motion is

$$m\ddot{z} + \gamma\dot{z} + kz = F_0 \cos \omega t + F_{ts}(d,i), \qquad (1)$$

where z is the position of the mass m, k is the spring constant, γ is the damping coefficient, F_0 is the magnitude of the driving force, ω is the drive frequency, $d(t)=d_0-z(t)$ is the instantaneous tip-sample separation, d_0 is the equilibrium tip-sample separation, and positive z is in the direction toward the sample. The tip-surface force $F_{ts}(d,i)$ depends on both d and the current state i of the tip-surface force interactions. There are three possible states: (1) long-range attraction; (2) long-range attraction, and capillary interactions; and (3) adhesion, capillary interactions, and repulsive contact with the surface.

The long-range attractive van der Waals force is modeled by

$$F_v = \begin{cases} \dfrac{HR}{6d^2} & d > a_0 \\[2mm] \dfrac{HR}{6a_0^2}d & d \leq a_0, \end{cases} \qquad (2)$$

where H is the Hamaker constant, R is the tip radius, a_0 is the intermolecular distance given by $a_0=\sqrt{H/24\pi\gamma_{sv}}$, and γ_{sv} is the surface energy of the tip and sample. The repulsive contact force is found using the Derjaguin–Muller–Toporov (DMT) model as

a)Electronic mail: nastaran@vt.edu.

104, 063518-1

$$F_r = -(4/3)E^* R^{1/2}(a_0 - d)^{3/2} d \le a_0, \tag{3}$$

where E^* is an effective Young's modulus of the tip and surface. The attractive capillary force is modeled by

$$F_c = \begin{cases} 4\pi\gamma_w R/(1 + d/h) d > a_0 \\ 4\pi\gamma_w R/(1 + a_0/h) d \le a_0, \end{cases} \tag{4}$$

where γ_w is the surface energy of water, and h is the thickness of the capillary water layer. For $d \le a_0$ the capillary force is assumed to remain at the constant value given at $d = a_0$. As the cantilever approaches the surface the capillary layers merge when $d = d_{on}$ where it is assumed that $d_{on} = 2h$. The capillary force remains until the liquid bridge or meniscus is broken when $d = d_{off}$. Using geometrical arguments and DMT theory yields $d_{off} = V^{1/3} - V^{2/3}/(5R)$, where the volume of the meniscus $V = 4\pi R h^2 + 4\pi h^3/3 + 2\pi r^2 h$ and $r = (3\pi\gamma_w R^2/E^*)^{1/3}$ is the radius of the circular contact area.[17,19]

The capillary force is strongly hysteretic $(d_{off} > d_{on})$ and yields the ambiguity in F_{ts} that necessitates its dependence on state. All of the tip-surface forces are conservative. This hysteresis is the only source of tip-surface dissipation. Any oscillation that breaks the capillary layer dissipates an equal and constant amount of energy given by

$$E_{tip} = 4\pi\gamma_w R h \ln\left(\frac{d_{off} + h}{3h}\right), \tag{5}$$

where E_{tip} is the area enclosed by the hysteresis loop of the force-distance curve. The power dissipated by breaking the meniscus is

$$P_{max} = E_{tip} f_0, \tag{6}$$

which is the maximum dissipation possible. f_0 is the frequency of oscillation and is assumed here to be the fundamental resonant frequency. The *exact* power dissipated for any complicated motion of the mass, for example, for chaotic or quasiperiodic dynamics, is the fraction f of the oscillations that break the meniscus

$$P_{tip} = f P_{max}, \tag{7}$$

where $0 \le f \le 1$. $f = 0$ is for solutions that never break the meniscus yielding $P_{tip} = 0$, and $f = 1$ is for solutions that break the meniscus every pass near the surface yielding $P_{tip} = P_{max}$. In the following we use parameter values for a Si cantilever tip and a Si surface:[17] $k = 27.5$ N/m, quality factor $Q = 400$, the beam is driven at its resonant frequency $f_0 = 280$ kHz, a free amplitude of oscillation of $A_0 = 21$ nm, $H = 6.0 \times 10^{-20}$ J, $R = 20$ nm, $\gamma_w = 72$ mJ/m^2, $E^* = 66$ GPa, and $a_0 = 0.1$ nm.

The energy dissipated is directly related to the difference between d_{off} and d_{on}, which is determined by γ_w, R, and h. As a result, P_{max} does not depend on the cantilever dynamics. Experimental measurements indicate that $h \approx 0.7$ nm corresponds to 100% relative humidity for a silicon surface.[18] Figure 1 shows P_{max} in the range of 0.1 nm $\le h \le 0.7$ nm. The solid line is the exact result from the model, and the dashed line is a curve fit given by $P_{max} \approx 4.5h^{0.71}$.

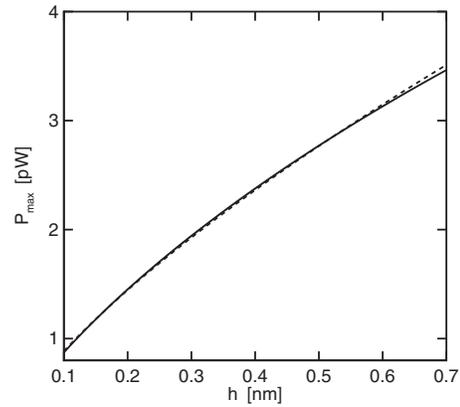The experimental system has rapidly changing tip-surface force interactions, which are not truly discontinuous.

FIG. 1. The variation in the maximum power dissipated P_{max} with the thickness of the capillary layer h. The solid line is the exact result. The dashed line is a curve fit given by $P_{max} \approx 4.5h^{0.71}$.

However, in order to draw physical insight from the mathematical model it is important to retain its features in the numerical simulations. We have performed simulations of Eq. (1) using the numerical techniques described in Ref. 16 that carefully treat the discontinuities and hysteresis in F_{ts}. We emphasize that artificially coarsening F_{ts} in the numerical approach would lead to errors in the values of f and thus an inaccurate determination of P_{tip}.

The inclusion of higher flexural eigenmodes of the cantilever, or of interactions with other modes of oscillation such as in-plane or torsional resonances, can lead to complex dynamics.[20–24] These additional eigenmodes are not necessary to capture the essential features of the power dissipated, and have not been included here. We focus on the power dissipated by the nonlinear dynamics of a single flexural mode interacting with a conservative and hysteretic force.

Using our numerical approach we compute precisely the fraction of trajectories f that break the meniscus to yield the exact power dissipated by Eq. (7). The variation in P_{tip} with d_0 is shown in Fig. 2 for a capillary film thickness of $h = 0.2$ nm. Figure 2 illustrates the low-amplitude or attractive solution, regions (1)–(5), and the high-amplitude or repulsive solution, region (6). The low-amplitude solution does not interact with the solid surface and experiences a net attractive force, whereas the high-amplitude solution interacts with the solid and experiences a net repulsive force. These coexisting solutions have been discussed in detail elsewhere.[16,17] Regions (1)–(5) form a dome that can be directly related to the cantilever dynamics. In region (1), $P_{tip} = 0$ and the capillary layer remains untouched. In region (2), the dynamics are quite complicated yet there is a simple trend in f, as shown in Fig. 3. For values of d_0 where the cantilever first breaks the meniscus f is quite small indicating that this occurs only in a small fraction of the time. Upon breaking the meniscus, an amount of energy E_{tip} is dissipated. As a result, it takes several oscillations for the cantilever to return to interacting with the capillary layer, upon which this cycle repeats (see Fig. 4). This trend continues as d_0 is reduced and f increases. Eventually a periodic solution is reached where every trajectory breaks the meniscus to yield the plateau labeled region (3) at $P_{max} = 1.45$ pW indicated by the dashed horizontal line. As d_0 decreases further the periodic dynamics terminate
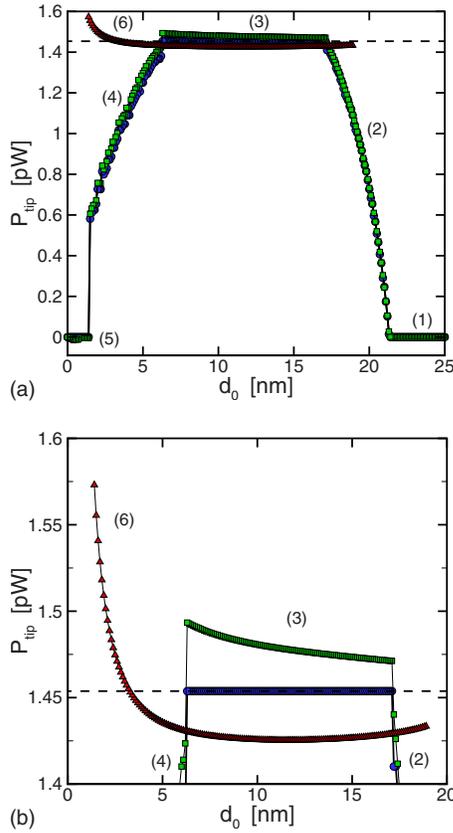
FIG. 2. (Color online) (a) The variation in P_{tip} with equilibrium tip-sample separation d_0 for a capillary layer thickness $h=0.2$ nm. Regions (1)–(5) are the low-amplitude solution. Region (6) is the high-amplitude solution. (b) A close-up view of the results in panel (a) near the plateau region. Blue circles are the exact value for the low-amplitude solution found using Eq. (7). Green squares are for the low-amplitude solution, and the red triangles are for the high-amplitude solution found using Eq. (8). Each symbol is the result of a single long-time numerical simulation, and the solid lines are included to guide the eye.

to a solution where the cantilever tip remains entirely *inside* the fluid layer for several oscillations before breaking the meniscus, indicated by region (4). The meniscus must be broken for energy to be dissipated. As a result, this also leads to a reduction in P_{tip}. As d_0 is decreased the fraction of oscillations remaining in the fluid layer increases. Eventually, this terminates and the cantilever exhibits a periodic solution where the tip never leaves the water layer yielding $P_{tip}=0$ indicated by region (5). These dynamics are general and are shown over a range of h in Fig. 2(b).

The magnitude of P_{tip} in regions (1), (3), and (5) can be predicted without knowledge of the cantilever dynamics whereas the dissipated power in regions (2) and (4) depend on the dynamics. The origin and termination of the five regions also depends on the dynamics. This is illustrated in Fig. 3(a) for low-amplitude solutions at different values of h. The rise and fall of f in regions (2) and (4), respectively, are similar over the range of capillary layer thicknesses explored [Fig. 3(a)]. To quantify these trends we give curve fits for regions (2) and (4) for $h=0.2$ nm, as shown by the solid lines in Figs. 3(b) and 3(c), which are $P_{tip} \approx -0.91+1.32d_0 -0.04d_0^2$ for 17.2 nm $\leq d_0 \leq 21.2$ nm and $P_{tip} \approx 1.87d_0^{0.62}$ for 1.5 nm $\leq d_0 \leq 6.2$ nm. As h increases the initial interaction with the fluid layer occurs at larger d_0 because $d_{on}=2h$ and
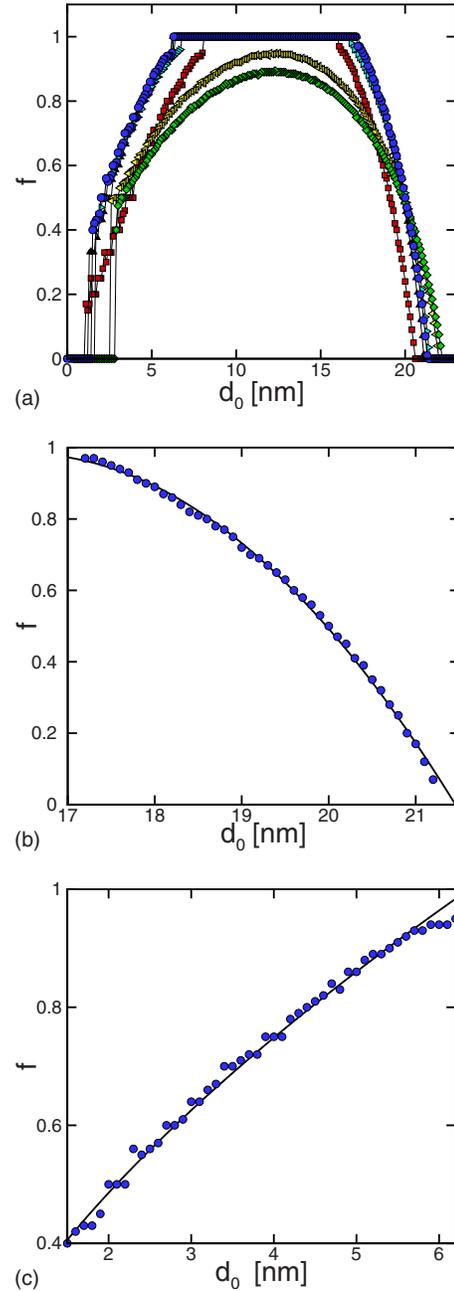

FIG. 3. (Color online) (a) The fraction f of trajectories that break the meniscus for different values of the capillary layer thickness: $h=0.1$ nm (red, squares), 0.15 nm (black, deltas), 0.2 nm (blue, circles), 0.25 nm (cyan, right triangles), 0.5 nm (yellow, left triangles), and 0.6 nm (green, diamonds). The width of the plateau region is shown in Fig. 5. (b) A detailed view of region (2) for $h=0.2$ nm. The blue circles are the results from numerical simulation and the solid line is a curve fit given by $P_{tip} \approx -0.91+1.32d_0-0.04d_0^2$ for 17.2 nm $\leq d_0 \leq 21.2$ nm. (c): A detailed view of region (2) for $h=0.2$ nm. Again the blue circles are from numerical simulation and the solid line is a curve fit given by $P_{tip} \approx 1.87d_0^{0.62}$ for 1.5 nm $\leq d_0 \leq 6.2$ nm.

shifts the origin of the plateau of region (3) to larger values of d_0. For $h \approx 0.45$ nm, region (3) disappears and a steady oscillating solution that breaks the meniscus every oscillation is never achieved. As a result $f<1$, as shown for $h=0.5$ and 0.6 nm. The nonlinear variation of the width of the plateau region (3) with increasing h is shown in Fig. 5.

To illustrate the complexity of the dynamics, Fig. 4(a) shows the cantilever velocity $\dot{z}$ as a function of position z for
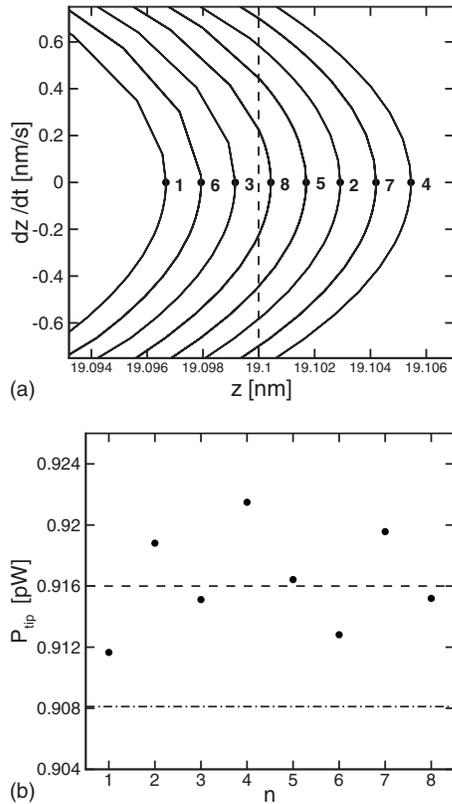
FIG. 4. (a) Velocity vs the position for a solution where $f=5/8$, i.e., the cantilever breaks the meniscus 5 out of every 8 passes. The dashed line indicates the location of the undisturbed capillary layer. Oscillations (1, 6, and 3) do not break the meniscus, and oscillations (8, 5, 2, 7, and 4) do break the meniscus. (b) P_{tip} for the trajectory shown in panel (a) as a function of the nth pass near the surface. The circles are found using the harmonic approximation of Eq. (8), and the dashed line is their average value. The dash-dotted line is the exact value of P_{tip}.

FIG. 5. The variation of the width w of the plateau given by region (3) in Fig. 2(b) as a function h. Symbols represent results from numerical simulation. The solid line is a seventh order polynomial fit to guide the eye. The plateau region vanishes at $h \approx 0.45$ nm.

retracting continues far past this location. Passes $n=1,6,3$ do not contact the capillary layer and passes $n=8,5,2,7,4$ enter the capillary layer and subsequently break the meniscus. In general, after breaking the meniscus the maximum value of z for the very next pass is reduced. Subsequent passes have increasing values of amplitude until the water layer is contacted again. In the case shown, these eight passes repeat in sequence and represent the steady oscillating solution. Similar dynamics are found over all of region (2). Furthermore, the same trends are found in region (4). In this case the energy dissipated by an oscillation that breaks the meniscus tends to cause subsequent oscillations to remain in the capillary layer due to the small values of d_0.

A commonly used approach in the experimental measurement of P_{tip} is to assume that the cantilever dynamics can be described by a single sinusoid with frequency equal to that of the drive to yield[4]

$$P_{tip} = \frac{kA^2\omega_0}{2Q}\left(\frac{A_0}{A}\sin\varphi - 1\right), \tag{8}$$

where it has been assumed that the cantilever is driven at resonance $\omega = \omega_0$. In practice, the values of the amplitude A and phase φ of oscillation used in Eq. (8) are often inputs given from experimental measurement. It has been shown for AFM cantilevers that the higher harmonics of the fundamental mode of oscillation are often excited and this can be used to gain useful information about the sample.[25–29] The higher harmonics could be included in the analysis to yield a more accurate description of the dynamics and therefore an improvement in Eq. (8). However, this requires not only periodic dynamics, but knowledge of the period of the dynamics, which is not necessarily known beforehand. For example, consider the situation where the cantilever dynamics repeat after several oscillations of the drive, i.e., the high-periodic dynamics characteristic of regions (2) and (4) of Fig. 3. Our results indicate that it may be possible to predict P_{tip} accurately even without this knowledge as indicated by the simple trend of f with d_0.

We emphasize that our approach only requires knowledge of f and, as a result, our calculations do not require periodic dynamics and remain valid for irregular motion. Upon breaking the meniscus, the model assumes that the fluid layers instantaneously return to their equilibrium positions. As a result, even if the period of the dynamics were known beforehand and the higher harmonics were included, these small corrections to the amplitude would not alter f, and therefore would not contribute to the power dissipated.

The nonlinearities from the contact and capillary models act for very short times and over very small portions of a cantilever oscillation. As a result, the dynamics remain nearly sinusoidal, and Eq. (8) yields only minor errors. Figure 2(a) compares P_{tip} found using Eq. (8) with the exact value from Eq. (7) for high and low-amplitude solutions. The high-amplitude solution, region (6), experiences the strong nonlinearity of the surface contact model and breaks the fluid meniscus at every oscillation. The resulting dissipation is exactly P_{max}. In this case, the strong nonlinearity of the contact model is significant and Eq. (8) deviates from the actual dissipation. Equation (8) underpredicts the dissipation and

the solution in region (2) with $f=5/8$ of Fig. 2(a). This is a close-up view of the cantilever trajectory as it comes closest to the surface. Each pass near the surface is labeled with a number n indicating the sequence in which the passes occur. The vertical dashed line represents the location of the undisturbed capillary layer. The location where the meniscus breaks is out of view to the left and every oscillation when
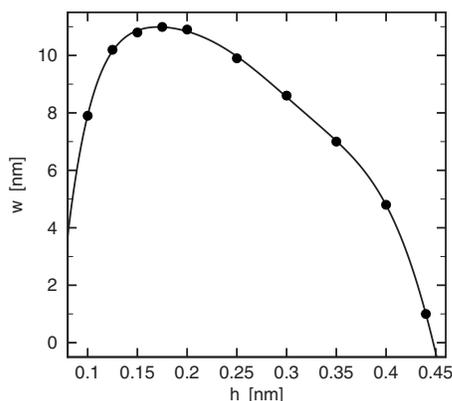
for very small values of d_0, where the influence of the contact repulsion is largest, it clearly leads to significant errors.

The low-amplitude solution only interacts with the long range attraction and capillary forces, and, in this case, Eq. (8) is quite accurate for the entire power dissipation-separation curve. For the plateau region, Eq. (8) slightly overpredicts the dissipation. It is interesting to consider further how Eq. (8) remains so accurate in regions (2) and (4) where many of the oscillations never actually break the meniscus layer and, as a result, do not contribute to the power dissipated. Figure 4(b) explores this further for the case of region (2) where $f = 5/8$ in Fig. 2(a). The symbols are the power dissipated using Eq. (8), where the amplitude and phase have been calculated at each of the n passes shown in Fig. 4(b). The average of these is what would typically be measured experimentally. This value is shown by the dashed line. The dash-dotted line represents the exact value as determined from our simulations. It is clear that Eq. (8) predicts a finite value of dissipation even for trajectories that do not break the meniscus. The value of the predicted dissipation reflects the magnitude of the amplitude for a particular pass. For example, passes $n = 1$ and 4 have the smallest and largest values of dissipation, respectively. Overall, the average of this response leads to a fairly accurate result.

In conclusion, our discussion is general for any hysteretic model with conservative forces yielding steady-state oscillating solutions. The fraction of trajectories experiencing hysteresis uniquely determines the power dissipated. Given an experimentally accurate model this could be used to probe the properties and dynamics of the fluid layer.[30] Furthermore, quantitative measurements of the dissipated power may provide a solid and unambiguous imaging tool for determining the morphology as well as the compositional variations of nanometric surface samples in an ambient environment.

ACKNOWLEDGMENTS

[1] B. Cappella and G. Dietler, Surf. Sci. Rep. **34**, 1 (1999).
[2] R. Garcia and R. Perez, Surf. Sci. Rep. **47**, 197 (2002).
[3] A. Raman, J. Melcher, and R. Tung, Nanotoday **3**, 20 (2008).
[4] J. P. Cleveland, B. Anczykowski, A. E. Schmid, and V. B. Elings, Appl. Phys. Lett. **72**, 2613 (1998).
[5] B. Anczykowski, B. Gostmann, H. Fuchs, J. P. Cleveland, and V. P. Elings, Appl. Surf. Sci. **140**, 376 (1999).
[6] M. Lee and W. Jhe, Phys. Rev. Lett. **97**, 036104 (2006).
[7] R. Garcia, C. J. Gomez, N. F. Martinez, S. Patil, C. Dietz, and R. Magerle, Phys. Rev. Lett. **97**, 016103 (2006).
[8] R. Garcia, R. Magerle, and R. Perez, Nat. Mater. **6**, 405 (2007).
[9] E. Sahagun, P. Garcia-Mochales, G. M. Sacha, and J. J. Saenz, Phys. Rev. Lett. **98**, 176106 (2007).
[10] B. Gotsmann, C. Seidel, B. Anczykowski, and H. Fuchs, Phys. Rev. B **60**, 11051 (1999).
[11] S. J. T. Van Noort, K. O. Van der Werf, B. G. De Grooth, N. F. Van Hulst, and J. Greve, Ultramicroscopy **69**, 117 (1997).
[12] H. Dankowicz, Philos. Trans. R. Soc. London, Ser. A **364**, 3505 (2006).
[13] N. A. Burnham, O. P. Behrendt, F. Oulevey, G. Gremaud, P.-J. Gallo, D. Gourdon, E. Dupas, A. J. Kulik, H. M. Pollock, and G. A. D. Briggs, Nanotechnology **8**, 67 (1997).
[14] R. Garcia and A. San Paulo, Phys. Rev. B **60**, 4961 (1999).
[15] K. Yagasaki, Phys. Rev. B **70**, 245419 (2004).
[16] N. Hashemi, M. R. Paul, and H. Dankowicz, J. Appl. Phys. **103**, 093512 (2008).
[17] L. Zitzler, S. Herminghaus, and F. Mugele, Phys. Rev. B **66**, 155436 (2002).
[18] D. Beaglehole and H. K. Christenson, J. Phys. Chem. **96**, 3395 (1992).
[19] C. D. Willett, M. J. Adams, S. A. Johnson, and J. P. K. Seville, Langmuir **16**, 9396 (2000).
[20] H.-J. Butt and M. Jaschke, Nanotechnology **6**, 1 (1995).
[21] M. Reinstaedtler, U. Rabe, V. Scherer, J. A. Turner, and W. Arnold, Surf. Sci. **532-535**, 1152 (2003).
[22] L. B. Sharos, A. Raman, S. Crittenden, and R. Reifenberger, Appl. Phys. Lett. **84**, 4638 (2004).
[23] Y. Song and B. Bhushan, Ultramicroscopy **106**, 847 (2006).
[24] Y. Song and B. Bhushan, Ultramicroscopy **107**, 1095 (2007).
[25] S. J. T. van Noort and O. H. Willemsen, Langmuir **15**, 7101 (1999).
[26] A. Sebastian, M. V. Salapaka, and D. J. Chen, J. Appl. Phys. **89**, 6473 (2001).
[27] M. Stark, R. W. Stark, W. M. Heckl, and R. Guckenberger, Proc. Natl. Acad. Sci. U.S.A. **99**, 8473 (2002).
[28] R. W. Stark, Nanotechnology **15**, 347 (2004).
[29] A. Sebastian, A. Gannepalli, and M. V. Salapaka, IEEE Trans. Control Syst. Technol. **15**, 952 (2007).
[30] H. Choe, M.-H. Hong, Y. Seo, K. Lee, G. Kim, J. Ihm, and W. Jhe, Phys. Rev. Lett. **95**, 187801 (2005).